

# Calculation of Measurement Errors in Research of Adhesion of Scale to the Steel Substrates for Cold Specimens

Jarosław Boryca<sup>1</sup> • Tomasz Wyleciał<sup>1</sup>

<sup>1</sup>*Department of Production Management, Czestochowa University of Technology, Faculty of Production Engineering and Materials Technology University, 42-200 Częstochowa, Al. Armii Krajowej 19, Poland, e-mail: jboryca@op.pl*

Category : Original Scientific Paper

Received : 12 December 2019 / Revised: 28 December 2019 / Accepted: 29 December 2019

*Keywords : Adhesion of scale, Cold sample method, Steel*

*Abstract : In experimental research, determining the potential measurement errors is an extremely important element. Also, the scale adhesion tests require such calculations. The paper presents the results of the scale adhesion tests for specific thermochemical parameters using the cold samples method. The calculation scheme and results of calculating measurement errors were also demonstrated.*

*Citation: Boryca Jaroslaw, Wylecial Tomasz : Calculation of Measurement Errors in Research of Adhesion of Scale to the Steel Substrates for Cold Specimens, Advance in Thermal Processes and Energy Transformation Volume 2, No.4 (2019), p. 61-64, ISSN 2585-9102*

## 1 Introduction

In the process of heating steel before plastic working, in addition to heat exchange-related processes, the processes of chemical interaction also occur between the furnace atmosphere and the surface of the steel being heated. As a result of oxidation, scale forms, which causes not only the losses of the heated material and slows down the heating process, but also adversely affects the service life of heating equipment. An important issue in the operation of heating furnaces is the adhesion of a scale layer to the surface of the steel being heated. Too high adhesion causes the scale not being completely removed from the surface of the heated charge and it is subsequently rolled into the surface of the product during the plastic working process. The removal of laps requires arduous and costly mechanical working [1÷3]. The problem of scale adhesion in heating process has been widely covered in publications [3÷10].

In scientific research, determining the value of measurement errors that can affect the quality of research is an extremely important element. The imperfections of the measuring apparatus, imperfections of observation and elusive influence of the environment may cause differences in the values of physical quantities determined by measurement and expressed by a specific number of units in relation to the actual value of this quantity. This difference is called an absolute error. The relative error of the

measurement is equal to the ratio of the absolute error to the actual value [11].

There are many reasons for the magnitude of the measurement error. Depending on the type of cause and the nature of the error, it decides whether these are systematic or accidental errors [11÷17]. Systematic errors always affect in the same way the result of a measurement carried out using the same measuring apparatus and method of measurement. Random errors are the result of many small and variable random factors.

## 2 Measuring stand and research methodology

To realize the objective of the research, a specialized laboratory has been built at the Department of Production Management. A combustion chamber with a gas burner are integrated with the furnace. The burner performs the role of a gaseous atmosphere generator. The value of excess air ratio, and thus the chemical composition of combustion gas, is regulated in the burner. The remaining thermal power of the furnace is supplied in the form of electric power, which allows the temperature to be precisely controlled at any location of the heating chamber of the furnace. The temperature in the furnace is controlled by means of a TROL – 9090 regulator. The accuracy of temperature control is  $\pm 1.0\text{K}$ . The furnace chamber temperature is measured by means of a PtRh-Pt control thermocouple and a NiCr-Ni measuring thermocouple. The value of

excess air ratio is controlled by the continuous measurement of the intensity of flow of gas and air supplied to the burner. The intensity of flow of gas and air is measured with rotameters [6÷8]. A schematic diagram of the furnace is shown in Figure 1.

down to ambient temperature, followed by joining the formed scale with reference samples using a glue of an appropriate tensile strength. The method applied to the testing of scale adhesion to the cold charge is a quantitative method allowing the numerical

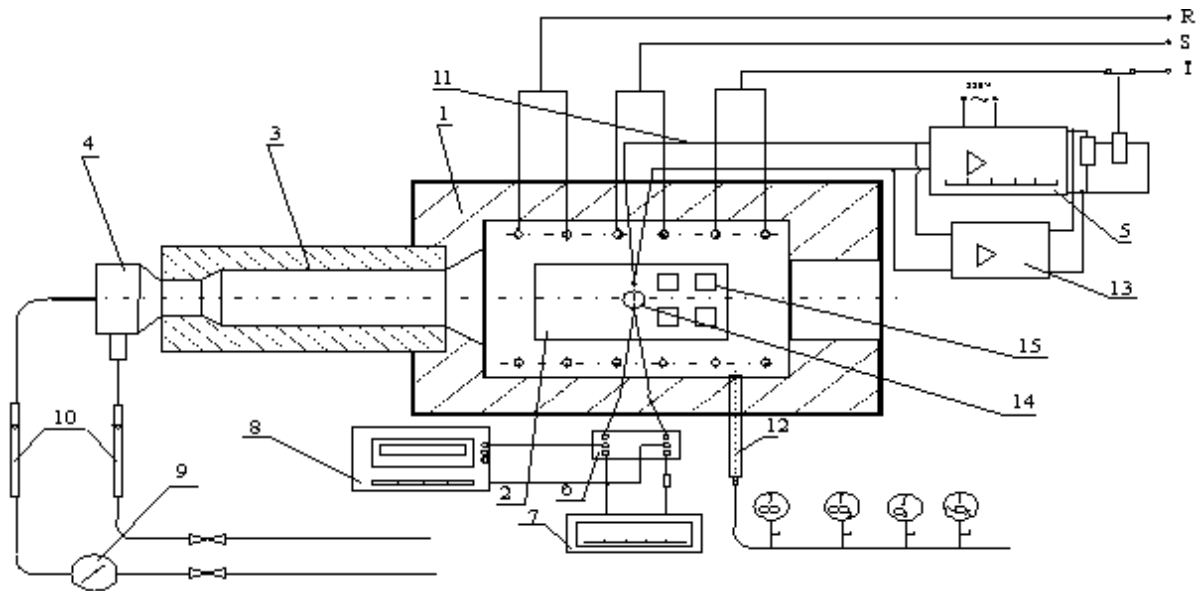


Figure 1 Schematic diagram of an electric&gas furnace [6, 18]

1 - furnace, 2 - refractory stand, 3 - combustion chamber, 4 - burner, 5 - temperature regulator, 6 - compensation box, 7 - temperature recorder, 8 - milivoltmeter, 9 - gas meter, 10 - rotameters, 11 - PtRh-Pt control thermocouple, 12 - combustion-gas drawing probe, 13 - programmable temperature controller, 14 - test specimen with a NiCr-Ni thermocouple, 15 - specimens tested

Measurements, for cold samples, were performed by measuring the force needed for detaching the scale layer and then by calculating the adherence ( $P_z$ ) expressed in MPa.

The value of the scale adhesion for cold method is defined by the following relationship:

$$P_z = \frac{Q_r}{A_{cz}} \cdot 10^{-6} \quad (1)$$

where:

$P_z$  - scale adhesion for cold method, (MPa),

$Q_r$  - value of force needed, (N),

$A_{cz}$  - field of surface of researched foremost sample, ( $m^2$ ).

It should be noted that the direct adhesion measurements were preceded by cooling the samples

determination of the force that bounds the scale with the steel core. The value of force needed for detaching the scale layer from the steel surface was measured by using a TC-FR100TL.A4K testing machine [6]. Scheme of course research present on Figure 2. Scheme of testing machine present on Figure 3.

### 3 Results of adhesion measurements

It carry measurements of masses of samples in the successive stages of the test. Calculation of scale adhesion on the base of carried measurements was executed. The heating were varied out with the value of combustion air excess ratio of  $\alpha=0.6\div1.4$ . and heated in temperature 900, 1000, 1100, 1200 and 1300°C. Results of measurements and accounts summarized in Table 1 and Table 2.

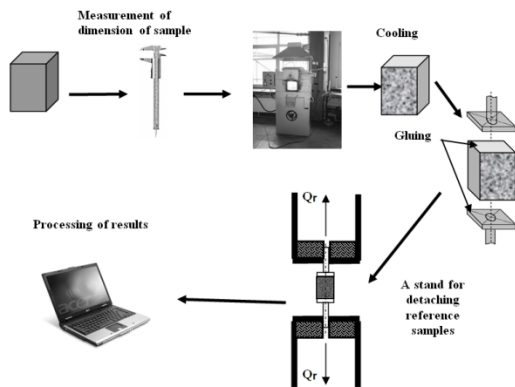


Figure 2 Scheme of course research of the scale adhesion [6]

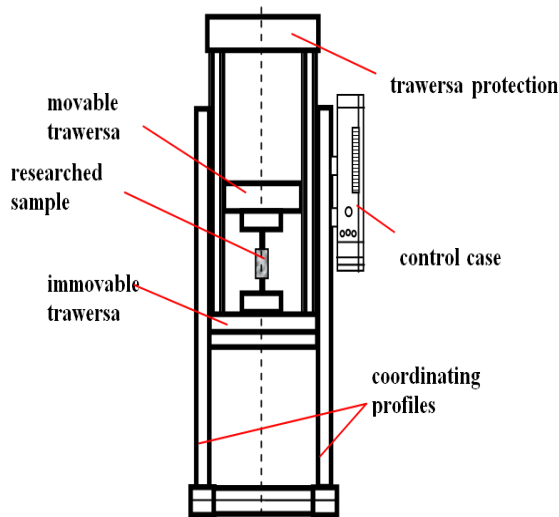


Figure 3 Scheme of testing machine

Table 1 The results of the measurements of scale adhesion  $P_z$  (MPa) for  $\alpha \leq 1.0$

Temperature $t$ [°C]	Value of combustion air excess ratio $\alpha$				
	0.6	0.7	0.8	0.9	1
900	0.545	0.646	0.748	0.852	0.956
1000	0.963	1.142	1.322	1.505	1.690
1100	1.567	1.857	2.150	2.448	2.749
1200	2.386	2.826	3.274	3.726	4.184
1300	3.443	4.079	4.724	5.378	6.038
1330	3.809	4.513	5.227	5.950	6.682

Table 2 The results of the measurements of scale adhesion  $P_z$  (MPa) for  $\alpha > 1.0$

Temperature $t$ [°C]	Value of combustion air excess ratio $\alpha$			
	1.1	1.2	1.3	1.4
900	1.085	1.169	1.251	1.332
1000	1.794	1.931	2.067	2.202
1100	2.755	2.966	3.175	3.381
1200	3.991	4.298	4.600	4.899
1300	5.517	5.941	6.359	6.772
1330	6.032	6.495	6.952	7.404

#### 4 Analysis of measurement errors

In the paper in the presented research, the cause of systematic errors can be:

- measurements of dimensions sample,  $\pm 10^{-5}$  m,
- measurements of the heating time,  $\pm 10$  s,
- accuracy of the temperature control,  $\pm 1$ K,
- accuracy of regulation of gas and air flow,  $\pm 10^{-2}$  m<sup>3</sup>.h<sup>-1</sup>.

To calculate  $\Delta P_z$ , for the scale adhesion determined by the cold method, the equation (1) should be written in the form:

$$\Delta P_z = \left| \frac{\partial P_z}{\partial Q_r} \right| \cdot |\Delta Q_r| + \left| \frac{\partial P_z}{\partial A_{cz}} \right| \cdot |\Delta A_{cz}| \quad [\text{Pa}] \quad (2)$$

where:

$$\Delta Q_r = \pm 1 \text{ N.}$$

The value of  $\Delta A_{cz}$  was calculated by means of the absolute differential method from the dependence on the surface of the square:

$$\Delta A_{cz} = \left| \frac{\partial A_{cz}}{\partial a} \right| \cdot |\Delta a| \quad [\text{m}^2] \quad (3)$$

After differentiation, we received:

$$\Delta A_{cz} = 2 \cdot a \cdot |\Delta a| = \pm 6 \cdot 10^{-6} \text{ m}^2 \quad (4)$$

Differentiating and substituting the results of calculations for the relationship (2) was obtained:

$$\Delta P_z = \frac{1}{A_{cz}} \cdot |\Delta Q_r| + \left(-\frac{Q_r}{A_{cz}^2}\right) \cdot |\Delta A_{cz}| = \pm 57 \text{ Pa} \quad (5)$$

The average value of the adhesion measure will be:

$$\bar{P}_z = \frac{\sum_{i=1}^n P_z}{n} = \frac{181.747}{54} = 3.366 \text{ MPa} \quad (6)$$

The average value of a relative systematic error is:

$$\delta_z = \frac{\Delta P_z}{\bar{P}_z} \cdot 100\% = 0.0017 \% \quad (7)$$

## 5 Conclusions

The accuracy of measurements can also be affected by accidental errors to which, in the case of the presented research, can be included:

- changes in ambient parameters,
- fluctuations in the chemical composition of the gas,
- fluctuations in gas pressure,
- fluctuations in air pressure,
- other.

Analyzing the obtained values of absolute statistical error and average relative error, it can be concluded that the measurement of the adhesion of the scale to the steel substrate for cold method has been carried out with high accuracy.

### The reference list

- [1] WAWRZYK P., WESSELY P.: *Bezzgorzelinowe nagrzewanie stali w piecach grzewczych*, „Śląsk”, Katowice 1973.
- [2] SZARGUT J., KOZIOŁ J., MAJZA E.: *Zasady poprawy eksploatacji pieców grzejnych*, Zeszyty Naukowe Pol. Śl., Energetyka z. 106., Gliwice 1989.
- [3] KIELOCH M.: *Energooszczędne i małożgorzelinowe nagrzewanie wsadu stalowego*, Prace naukowe Wydziału Inżynierii Procesowej, Materiałowej i Fizyki Stosowanej, Seria Metalurgia nr 29, Częstochowa 2002.
- [4] HIGGINSON R. L., ROEBUCK B., PALMIERE E. J.: *Texture development in oxide scales on steel substrates*, Scripta Materialia 2002, No. 47, pp. 337-342.
- [5] GOLIS B., PILARCZYK J. W., BŁAŻEJOWSKI Z.: *Druty stalowe*, Politechnika Częstochowska, Prace dydaktyczne, Seria Metalurgia No. 35, Częstochowa 1991.
- [6] BORYCA J.: *Przyczepność warstwy żgorzeliny powstałej w procesie nagrzewania wsadu stalowego*, Praca doktorska, Politechnika Częstochowska, Częstochowa 2005.
- [7] BORYCA J., KIELOCH M., PIECHOWICZ Ł.: *Investigation of the adhesion of scale forming in the process of steel charge heating before plastic working*, Archives of Metallurgy and Materials, Vol. 51, No. 3, pp. 451-457, 2006.
- [8] KIELOCH M., BORYCA J., PIECHOWICZ Ł.: *Przyczepność żgorzeliny w procesie nagrzewania wsadu stalowego*, Hutnik 2005, No. 1, pp. 7-12.
- [9] BORYCA J., WYLECIAŁ T., URBANIAK D.: *The Effect of Condition of the Charge Surface on the Scale Adhesion for Excess Air Combustion*, Metalurgija, Vol. 54, No. 1, s. 83-86, 2015.
- [10] BORYCA J., KIELOCH M., PIECHOWICZ Ł.: *Analysis of influence of heating time on the scale adhesion to the steel surface*, Acta Metallurgica Slovaca, Vol. 13, No. 3, pp. 52-57, 2007.
- [11] KOTLEWSKI F.: *Pomiary w technice cieplnej*, WNT, Warszawa 1972.
- [12] KULESZA J.: *Pomiary cieplne*, WNT, Warszawa 1993.
- [13] RYSZKA E.: *Pomiary zapylenia gazów w przewodach*, „Śląsk”, Katowice 1972.
- [14] STRZAŁKOWSKI A., ŚLIŻYŃSKI A.: *Matematyczne metody opracowywania wyników pomiarów*, PWN, Warszawa 1969.
- [15] MICHAŁOWSKI M., CIUBA Z., MACHNIEWICZ J., ZIĘBA A.: *Badania i pomiary cieplne pieców w hutnictwie żelaza*, „Śląsk”, Katowice 1973.
- [16] HANSEL H.: *Podstawy rachunku błędów*, WNT, Warszawa 1968.
- [17] ROMANOWSKI Ś., WRONA W.: *Matematyka wyższa dla studiów technicznych - część I*, PWN, Warszawa 1967.
- [18] BORYCA J., KIELOCH M.: *The adhesion of scale to the steel substrate in the process of heating the charge before plastic working*, Acta Metallurgica Slovaca Vol. 8, No. 4, pp. 20- 28, 2002.

# A Comparison of the Calculation Methods for Inflow Curves Creation to Software Prosper

Branislav Halek<sup>1</sup> • Dávid Heinz<sup>2</sup>

<sup>1</sup>Department of Montaneous Sciences, Technical University of Košice, Letná 9, 040 01 Košice, Slovak Republic, branislav.halek@tuke.sk

<sup>2</sup>Institute of logistics and transport, Technical University of Košice, Letná 9, 040 01 Košice, Slovak Republic, david.heinz@tuke.sk

Category : Review Article

Received :22 December 2019 / Revised:29 December 2019 / Accepted:30 December 2019

Keywords : Inflow Performance Relationship, Vogel equation, Darcy equation, Software Prosper

**Abstract :** The oil reservoir behavior and evaluation of its deliverability belongs to the fundamental role of production engineers in the petroleum industry. The ability of the well to produce is characterized by the relationship between the total liquid flow rate and bottom-hole flowing pressure. This relationship is so-called IPR – inflow performance relationship. Nowadays, there are many different IPR correlations in petroleum industry but the most common use model is Vogel's method. With the development of computer technology were created computer softwares for this purpose. In this article, Prosper 14.0 was used to compare the results obtained by manual calculation using the Vogel's method. At the same time, a manual calculation based on Darcy's reservoir model was created and compared with the software in which it was used as the main reservoir model.

**Citation:** Halek Branislav, Heinz Dávid: A Comparison of the Calculation Methods for Inflow Curves Creation to Software Prosper, Advance in Thermal Processes and Energy Transformation, Volume 2, No. 4, (2019), p. 65-70, ISSN 2585-9102

## 1 Introduction

One of the most important components of the entire production system is reservoir. If it is not possible to predict current and future liquid flow rate into the well, the entire system cannot be analyzed. The flow into the well depends on the drawdown or pressure drop in the reservoir ( $\Delta p$ ). The pressure drawdown is characterized as a difference between reservoir pressure ( $P_R$ ) and bottom-hole flowing pressure ( $P_{wf}$ ). The relationship between drawdown and liquid flow rate ( $Q$ ) occurring in the porous medium depends on many parameters such as rock properties, fluid properties, compressibility of the flowing fluids, fluid saturations in the rock, reservoir energy. In petroleum terminology, this relationship is graphically illustrated and named as inflow curves [1]. The simplest shape of the inflow curves is a straight line in the undersaturated oil reservoir ( $P_R > P_b$ ). The inflow into a well is directly proportional to the pressure drawdown and the constant of proportionality is the productivity index (PI or J). The numerical value of the productivity index is given by the ((7), (8)) or under Darcy's law by ((15)), from the flowing bottom-hole pressures and flow rates measured during production tests. Its calculations are only suitable for undersaturated reservoir because variables that affect the productivity index and in turn

the inflow performance are the pressure-dependent parameters, e.g.: oil permeability ( $k_o$ ), oil viscosity ( $\mu_o$ ) and oil formation volume factor ( $B_o$  or FVF). Above the  $P_b$ , the term ( $k_o/\mu_o B_o$ ) from ((15)) is almost constant. As the pressure drops below the bubble point pressure, the dissolved gas is released from solution and the gas bubbles form in pores which can cause a large decrease this term. The overall effect of changing the pressure on this term is illustrated in (Figure 1)[2].

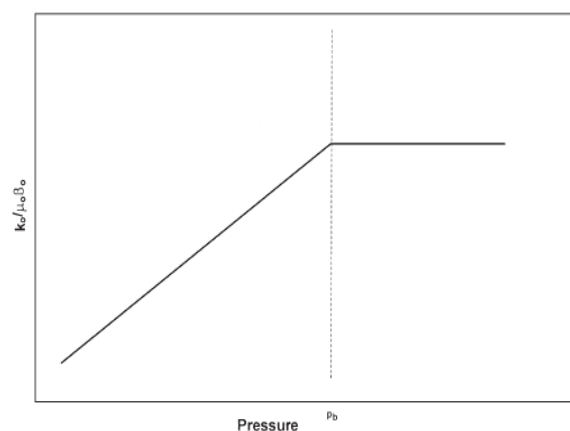


Figure 1 The term ( $k_o/\mu_o B_o$ ) as a function of pressure

Evinger and Muskat (1942) observed that when the pressure drops below the  $P_b$ , the inflow curve deviate from the simple straight-line relationship (Figure 2)[3].

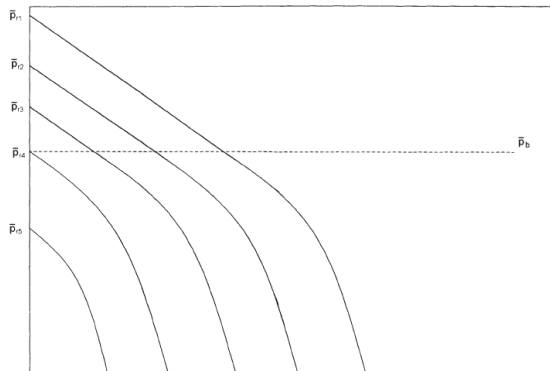


Figure 2 Effect of reservoir pressure

The flow from the reservoir into a well has been called inflow performance by Gilbert (1954). The Gilbert methodology was used to determination of well productivity by W.T.Weller (1966), who proposed a method to calculate the decline tendency of reservoir based on bottom-hole pressure and production rate[4]. The development and analysis of the first method to generate IPR's was carried out by Vogel, who made an important innovation to Weller's method, incorporating dimensionless terms. The other expressions for the inflow curves currently in use: M.B.Standing, M.J.Fetkovich, M.L.Wiggins, M.A.Klins and L.Clark.

## 2 Methods

The use of the IPR curves began in the middle of the 20th century to establish practical criteria for the exploitation of hydrocarbon reservoirs. The techniques used in these methods were based on the results of analyzes from real reservoirs. Currently, there are several basic methods for creating inflow curves based on earlier studies. The main essence of all empirical methods is:

- Using the stabilized flow test data, construct the IPR curve at the current reservoir pressure,
- Predict future inflow performance relationship as to the function of reservoir pressure.

The Vogel's research was developed by using the reservoir model proposed by Weller [5]. The resulting expression was based on calculations made from 21 different reservoirs, from which a dimensionless pressure and dimensionless oil flow rate, was developed [6].

$$\frac{Q}{Q_{max}} = 1 - 0,2 \left( \frac{P_{wf}}{P_R} \right) - 0,8 \left( \frac{P_{wf}}{P_R} \right)^2 \quad (1)$$

Standing noted that Vogel's equation can be extended by introducing the productivity index in order to predict future inflow performance relationship [7].

$$Q_f = \frac{J_f P_{Rf}}{1,8} \left[ 1 - 0,2 \left( \frac{P_{wf}}{P_{Rf}} \right) - 0,8 \left( \frac{P_{wf}}{P_{Rf}} \right)^2 \right] \quad (2)$$

where the subscript (f) refers to future condition.

The development of the inflow curve equation was based on 40 different oil wells from 6 different reservoirs. Fetkovich proposed a method for calculating the IPR for oil wells using the same type of equation that has been used for gas wells [8].

$$Q = C(P_R^2 - P_{wf}^2)^n \quad (3)$$

where:

C – performance coefficient (determined from production test data);

n – exponent depending on well characteristics (the value is ranged from 0,568 to 1).

Wiggins used principles of relative permeability and fluid physical properties as a basic input for the development of the IPR equation. His suggested relation is similar to Vogel's expression [9].

$$\frac{Q}{Q_{max}} = 1 - 0,52 \left( \frac{P_{wf}}{P_R} \right) - 0,48 \left( \frac{P_{wf}}{P_R} \right)^2 \quad (4)$$

The resulting expression is similar in form to that of Vogel's. Klins and Clark proposed to improve the predictive capability of Vogel's equation by introducing a new exponent (d). The final equation is [10]:

$$\frac{Q}{Q_{max}} = 1 - 0,295 \left( \frac{P_{wf}}{P_R} \right) - 0,705 \left( \frac{P_{wf}}{P_R} \right)^d \quad (5)$$

where:

$$d = \left[ 0,28 + 0,72 \left( \frac{P_{wf}}{P_R} \right) \right] (1,24 + 0,001 P_b) \quad (6)$$

## 3 Calculation

The reservoir deliverability depends on the efficient use of reservoir energy, which allows the fluid flow from the underground reservoir to the wellbore, separator and ultimately to the stock tank. The monitoring of the inflow to the wellbore is determined as the functional dependence of the flow rate and the pressure drawdown ( $Q = f(\Delta p)$ ), also known as the

inflow performance relationship. One of the most common used methods of constructing inflow curves is Vogel's method. The calculation algorithm by this method for a given reservoir type ( $P_R > P_b$ ) is:

- 1) Calculation of productivity index by using the stabilized test data point ( $Q$  and  $P_{wf}$ ). When recorded stabilized  $P_{wf}$  is less than the  $P_b$ :

$$J = \frac{Q}{(P_R - P_b) + \frac{P_b}{1.8} \left[ 1 - 0.2 \frac{P_{wf}}{P_b} - 0.8 \left( \frac{P_{wf}}{P_b} \right)^2 \right]} \quad (7)$$

when recorded stabilized  $P_{wf} \geq P_b$ :

$$J = \frac{Q}{P_R - P_{wf}} \quad (8)$$

- 2) Calculation of oil flow rate at the bubble point pressure:

$$Q_b = J(P_R - P_b) \quad (9)$$

- 3) Generation of IPR values above the  $P_b$  by different values of  $P_{wf}$  ( $P_{wf} > P_b$ ):

$$Q = J(P_R - P_{wf}) \quad (10)$$

Generation of IPR values below the  $P_b$  by different values of  $P_{wf}$  ( $P_{wf} < P_b$ ):

$$Q = Q_b + \frac{JP_b}{1.8} \left[ 1 - 0.2 \left( \frac{P_{wf}}{P_b} \right) - 0.8 \left( \frac{P_{wf}}{P_b} \right)^2 \right] \quad (11)$$

- 4) Calculation of maximum oil flow rate ( $Q_{max}$ ), when the  $P_{wf}$  is zero:

$$Q_{max} = Q_b + \frac{JP_b}{1.8} \quad (12)$$

- 5) Calculation of future oil flow rate at the specified future reservoir pressure. It consists of two steps:

Step 1. Calculate  $Q_{maxf}$  at  $P_{Rf}$ :

$$(Q_{max})_f = (Q_{max}) \left( \frac{P_{Rf}}{P_R} \right) \left[ 0.2 + 0.8 \left( \frac{P_{Rf}}{P_R} \right) \right] \quad (13)$$

Step 2. Calculate  $Q_f$  at different values of  $P_{wf}$ :

$$Q_f = (Q_{max})_f \left[ 1 - 0.2 \frac{P_{wf}}{P_{Rf}} - 0.8 \left( \frac{P_{wf}}{P_{Rf}} \right)^2 \right] \quad (14)$$

where subscript (f) represent future conditions.

Darcy's IPR model for undersaturated oil reservoir is based on the calculation of the oil flow rate using Darcy's equation for bottom-hole flowing pressure above bubble-point pressure, and the use of the Vogel's equation for  $P_{wf}$  below the  $P_b$ . This model is

also the most widely used in software Prosper in view of reservoir behavior in the future because it contains wider reservoir characteristics. The calculation procedure is the following:

- 1) Calculation of productivity index:

$$J = \frac{2\pi k_o h}{\mu_o B_o \ln \left( \frac{r_e}{r_w} \right)} \quad (15)$$

where:

$h$  – thickness (m);

$r_e$  – drainage radius (m);

$r_w$  – wellbore radius (m).

- 2) Generation of IPR values above the  $P_b$  by different values of  $P_{wf}$  ( $P_{wf} > P_b$ ):

$$Q = J(P_R - P_{wf}) = J\Delta p \quad (16)$$

- 3) Calculation of  $Q_{max}$  by using the stabilized test data point ( $Q$  and  $P_{wf}$ ):

$$Q_{max} = \frac{Q}{1 - 0.2 \left( \frac{P_{wf}}{P_R} \right) - 0.8 \left( \frac{P_{wf}}{P_R} \right)^2} \quad (17)$$

- 4) Generation of IPR values below the  $P_b$  by different values of  $P_{wf}$  ( $P_{wf} < P_b$ ):

$$Q = Q_{max} \left[ 1 - 0.2 \left( \frac{P_{wf}}{P_R} \right) - 0.8 \left( \frac{P_{wf}}{P_R} \right)^2 \right] \quad (18)$$

- 5) Calculation of future oil flow rate at the specified future reservoir pressure consists of two steps:

Step 1. For  $P_{wf} > P_b$ :  $P_R$  is replaced by  $P_{Rf}$  in ((16)).

Step 2. For  $P_{wf} < P_b$ : ((13), (14)) are used.

Based on the above calculations, we are able to construct the inflow curve at the current reservoir pressure and to predict the future behavior of the given reservoir, when the reservoir pressure drops. These calculations are a great help to the production engineers because pressure drop is necessary and irreversible part of reservoir life. If we can predict the future oil flow rate, we can correctly use a secondary or tertiary recovery method, sometimes referred to as enhanced oil recovery.

## 4 Results

In this article, the manual calculations of the inflow curve at the current reservoir pressure and its decrease according to the Vogel's and Darcy's methods are compared with software Prosper 14.0. The data

necessary for their construction can be found in Table 1.

Table 1 Input data

$P_R$	35,8	MPa
$P_b$	23,8	MPa
$P_{wf}$	16	MPa
$Q$	3375	$m^3 \cdot 24hod^{-1}$
$k_o$	$5,1 \cdot 10^{-14}$	$m^2$
$\mu_o$	$3,9 \cdot 10^{-4}$	Pa.s
$B_o$	1,41	$m^3 \cdot m^{-3}$
$R_e$	802,6	m
$R_w$	0,1079	m
$T$	98,8	$^{\circ}C$

where  $T$  is a reservoir temperature.

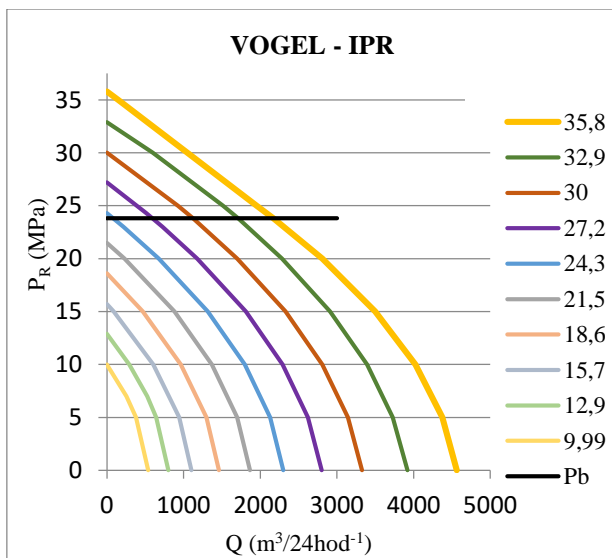


Figure 3 Vogel's inflow performance relationship

The calculations, in this case (Figure 3), consists of the equations ((7)-(14)). The oil reservoir is undersaturated, which determines the value of reservoir pressure that is higher than the bubble point pressure. Four dates are required to process the calculation: reservoir pressure, bubble-point pressure, stabilized bottom-hole flowing pressure, stabilized oil flow rate. A total of 10 inflow curves were constructed at a current reservoir pressure value 35,8MPa, up to a value of reservoir pressure 9,99MPa.

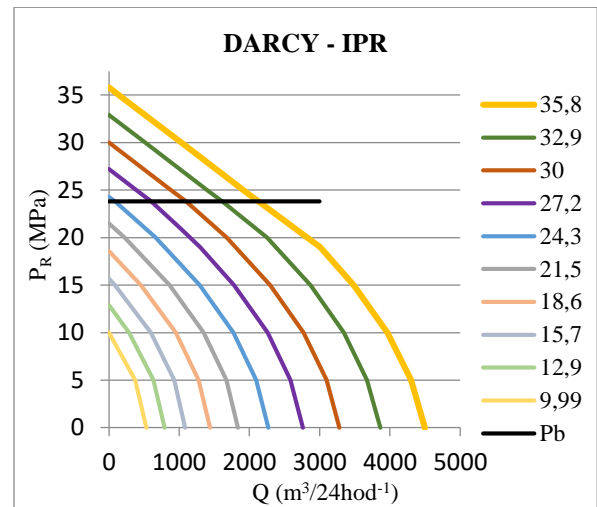


Figure 4 Darcy's inflow performance relationship

The calculation was performed at the same reservoir pressure value to be able to compare their results. Equations ((13)-(18)) were used to process the results. The data required for the calculation are shown in (Table 1). The resulting values of the total oil flow rate according to Vogel's and Darcy's methods are shown in (Table 2). To verify the results, the inflow curves were created in Prosper 14.0, which is a part of most petroleum companies today. Therefore, the resulting value obtained from this software will be considered as initial values. The design section of the software is shown in the (Figure 5) and the resulting inflow curves in the (Figure6).

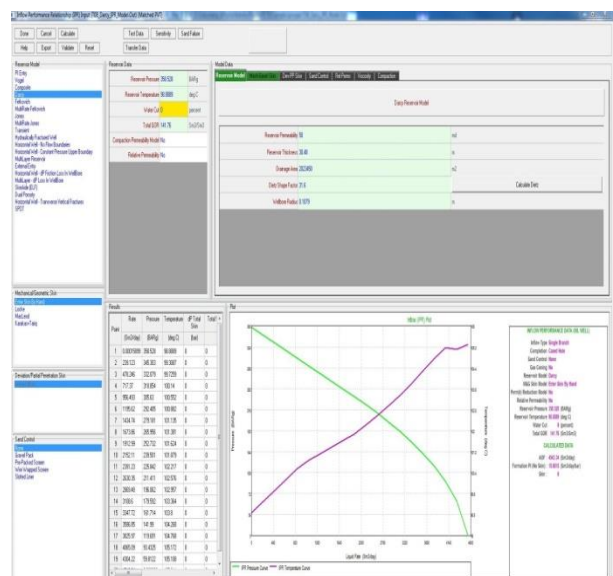


Figure 5 The Prosper IPR input screen

## 5 Discussion

Based on the above results in (Table 2), we can say that in manual calculations of inflow curves we make a maximum error in both cases of approximately 30%. At the specified 10 reservoir pressure values, the error increases by about 4%. The main factor affecting the accuracy of the results in the first case (Vogel) is the value of bubble-point pressure. In manual calculations, a constant value of  $P_b$  is used, but this value is, in fact, dependent on the reservoir temperature change. The change of  $P_b$  value is indicated by a red box in (Figure 7). As in the first method, also in the second (Darcy), the main factor of the errors is a change of values depending on pressure and temperature. In this case, the change of the  $P_b$  will be supplemented by the changes of  $\mu_o$  and  $B_o$ , used in the equation. This change of values is indicated in the (Figure 7) by a blue box.

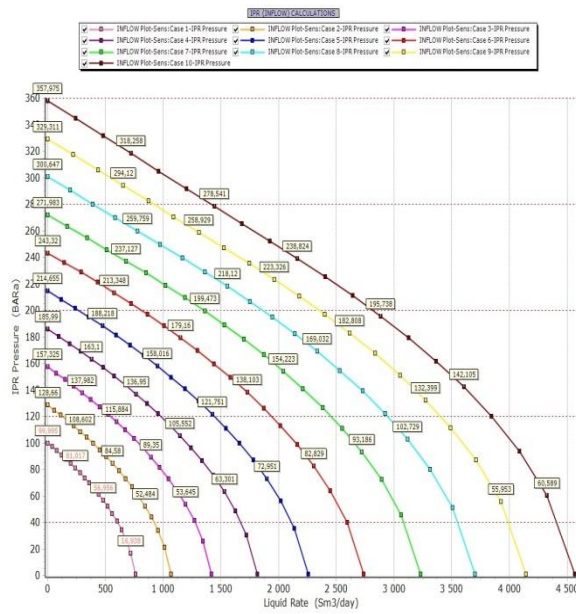


Figure 6 The Darcy IPR model in Prosper

Table 2 The resulting values of Q and calculation errors

$P_R$ (MPa)	$Q_{max}$ (P)	$Q_{max}$ (V)	Error (%)	$Q_{max}$ (D)	Error (%)
35,8	4543	4561	0,39	4495	1,1
32,9	4100	3920	4,6	3863	5,8
30	3650	3327	9	3279	10,1
27,2	3280	2799	14,7	2759	16
24,3	2700	2300	14,9	2267	16,1
21,5	2250	1864	17,2	1837	18
18,6	1800	1459	19	1438	20
15,7	1450	1102	24	1086	25
12,9	1050	802	24	791	25
9,99	750	539	28	531	29

where:

P – Prosper model;

V – Vogel’s method;

D – Darcy’s method;

Q – total oil flow rate ( $m^3 \cdot 24 \text{hod}^{-1}$ ).

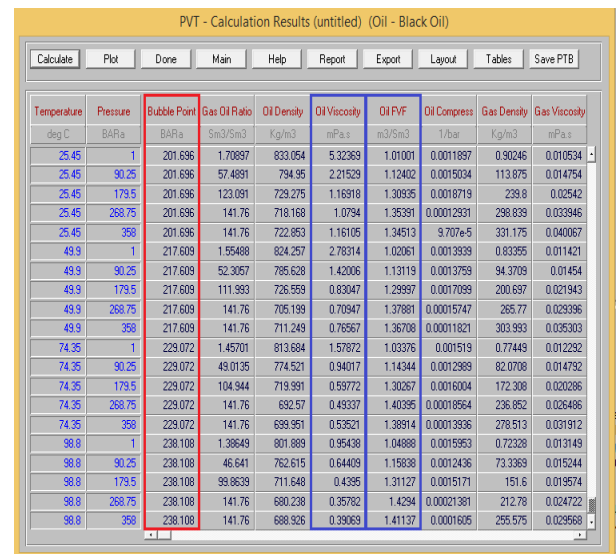


Figure 7 Change of  $P_b$ ,  $\mu_o$ ,  $B_o$  values obtained from software Prosper

Considering that the Darcy’s method, since a wider reservoir characteristic is used (15), the resulting error will be less than in the first case (Vogel), a comparative analysis of the selected values of  $P_R$  and  $P_{wf}$  in the Darcy method was performed with the software Prosper (Figure 8), (Table 3). By performing this analysis, it was found that for  $P_{wf} > P_b$  the maximum error was 2,7%, but for  $P_{wf} < P_b$  the maximum error was significantly greater (16,4%). Based on this fact, we can conclude that the measurement inaccuracy in the Darcy method occurs mainly when the  $P_{wf}$  falls below the  $P_b$ , when the Vogel equations are used ((13), (14)).

Table 3 The resulting values of  $Q$  and calculation errors

$P_R$ (MPa)	$P_{wf}$ (MPa)	$Q$ (P)	$Q$ (D)	Error (%)
35,8	25	1950	1914	1,9
32,9	25	1420	1400	1,5
30	25	910	886	2,7
27,2	25	400	390	2,5
$P_R$ (MPa)	$P_{wf}$ (MPa)	$Q$ (P)	$Q$ (D)	Error (%)
35,8	10	4020	3963	1,5
32,9	10	3600	3342	7,1
30	10	3125	2768	11,5
27,2	10	2700	2258	16,4

Prosper begins at a low level, but by gradually decreasing the reservoir pressure, the errors increases. Therefore, both methods offer good results of the oil flow rate in the early stage of well life. The main reason for the inaccuracies is that when the  $P_{wf} < P_b$ , the Vogel's equations in both cases are used. The resulting errors are also due to the fact that the used software Prosper takes into account any minimal changes in the physical properties of liquid and gaseous hydrocarbons as a function of the change in pressure and temperature.

**The reference list**

[1] BEGGS, H.: *Production optimization using nodal™ analysis*, Oklahoma, Copyright, 1991.

[2] AHMED, T.: *Reservoir engineering handbook*, Elsevier, 2010

[3] EVINGER, H.H., MUSKAT, M.: Calculation of theoretical productivity factors, *Trans.AIME*, pp. 126-146, 1942.

[4] GILBERT, W.E.: Flowing and gas-lift well performance, *API drilling and production practise*, New York, 1 January, 1954.

[5] WELLER, W.T.: Reservoir performance during two-phase flow, *J.petrol.technol.*, pp. 240-246, 1966.

[6] VOGEL, J.V.: Inflow performance relationship for solution gas drive wells, *Journal of petroleum technology*, January, 1968.

[7] STANDING, M.B.: Inflow performance relationship for damaged wells producing by solutions-gas drive, *J.petrol.technol.*, Vol. 22, pp. 1399-1400, 1970.

[8] FETKOVICH, M.J.: The isochronal testing of oil wells, Society of petroleum engineers, Dallas, pp.7, 1973.

[9] WIGGINS, M.L.: Generalized inflow performance relationship for three-phase flow, *Proceeding of the SPE production operations symposium*, USA, pp. 275-286, 1993.

[10] KLINS, M.A., CLARK, L.: An improved method to predict future IPR curves, *SPE reserv.eng.*, Vol.8, pp. 243-248, 1993.

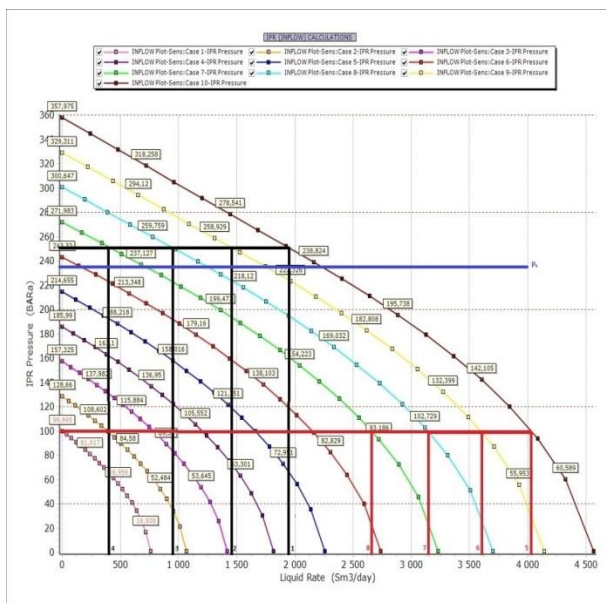


Figure 8 The Darcy IPR model in Prosper with selected values of  $P_R$  and  $P_{wf}$

**6 Conclusion**

In view of the above results, analyzes and comparisons, the following findings can be made. Creating of inflow curves by manual calculations of Vogel's method, the resulting values of the oil flow rate differ from the values obtained by modeling in software Prosper in the range from 0,39% to 28%. Using the Darcy's method the errors are roughly at the same level (1,1-29%). As in the first method and in the second, the variation of the obtained results with the

# Mathematical Model of Electrical Cabinet Cooling

Mária Polačiková<sup>1</sup> • Andrej Kapjor<sup>2</sup> • Milan Malcho<sup>3</sup> • Patrik Nemec<sup>4</sup>

<sup>1</sup>Department of Power Engineering, University of Žilina, Univerzitná 1, 010 26 Žilina, Slovakia, maria.polacikova@stroj.uniza.sk

<sup>2</sup>Department of Power Engineering, University of Žilina, Univerzitná 1, 010 26 Žilina, Slovakia, andrej.kapjor@stroj.uniza.sk

<sup>3</sup>Department of Power Engineering, University of Žilina, Univerzitná 1, 010 26 Žilina, Slovakia, milan.malcho@stroj.uniza.sk

<sup>4</sup>Department of Power Engineering, University of Žilina, Univerzitná 1, 010 26 Žilina, Slovakia, patrik.nemec@stroj.uniza.sk

Category : Original Scientific Paper

Received : 14 December 2019 / Revised: 27 December 2019 / Accepted: 28 December 2019

*Keywords* : heat pipe, mathematical model, operating temperature in electrical engineering

*Abstract* : The article focuses on cooling systems in electrical engineering, which are an interesting area of exploration and discovery. Specifically, it focuses on the mathematical calculation of cooling in electrical engineering. Cooling was provided by a heat pipe, which represents an interesting way of heat removal. The first part describes the origin and effect of elevated temperature in electrical equipment. The second part deals with the proposed procedure of calculating the mathematical model in cooling. This calculation relates to cooling by heat pipe at different volumes of working substance and at different temperature loads. The aim was to design a mathematical model by means of which the amount of heat removed from the heat pipe is calculated. The results of this model give theoretical information on the amount of heat removed.

*Citation*: Polačiková Mária, Kapjor Andrej, Malcho Milan, Nemec Patrik: Mathematical Model of Electrical Cabinet Cooling, Advance in Thermal Processes and Energy Transformation Volume2, No. 4, (2019), p. 71-75, ISSN 2585-9102

## 1 Introduction

The current development in the field of electrical engineering offers increasingly higher operational performance. The new, modern product design also wants to save space. Therefore, when it comes to electrical equipment that needs to be cooled, the question arises: how to ensure the cooling process of these equipment in the most efficient and energy saving way? There is a space for exploring and experimenting on this issue.

## 2 Heat loss

The heat generated by electrical conductors and electronic circuits is defined as the lossy Joule heat. It is also known as resistive or ohmic heat. It is one of the energy losses that cause overheating of electrical equipments. As a result of losses on the conductor and electrical components, heat is generated and that is

dissipated from the surface to the environment. The amount of heat dissipation depends in particular on the conductor core material, the type and size of the electrical equipment and the magnitude of the electric current. Joule's heat is proportional to the performance of the electrical equipment [1].

Maintaining the required operating temperatures in electrical equipment is an important condition for the correct operation of these equipment. Optimum operating conditions can be maintained with different types of cooling equipment. When designing these cooling systems in electrical engineering, great emphasis is placed on interior temperature and relative humidity. The reason is to create a safe environment for all electrical equipment. Electrical cabinets are designed to prevent dirt, dust and water from entering. The basic design criterion is the permissible operating temperature inside the core of the driver. The cross-sectional dimension of the conductor directly affects

the resistance of the line and thus the amount of heat generated. Excess heat is undesirable [2].

Manufacturers determine the maximum operating temperature of electrical components installed inside the equipment, typically at 50°C. When designing the cooling of electrical enclosures, a temperature of approximately 10°C below the maximum allowable temperature is considered. This extends the life of the device and minimizes the risk of overheating. The most common air temperature inside the electrical enclosure is 35°C. It is a compromise between the life of the components used and the way of cooling [2,3].

An example of a temperature-dependent lifetime for electrical equipment may be a capacitor. It has become one of the most commonly used components in electrical engineering. Its lifetime depends mainly on the temperature. The table 1 shows values that confirm the significant effect of temperature on the length of the proper functioning of the capacitor [4].

Table 1 Capacitor life dependence on ambient temperature [4]

Ambient temperature [°C]	Number of years of service life
45	32
55	16
80	4

Various types of cooling are used to create optimal operating conditions. The primary goal of any cooling system is to increase the performance and reliability of the chilled modules. There are various air or liquid cooling devices for heat dissipation in electrical engineering. Air cooling is one of the simplest cooling methods most commonly used for various electrical systems. The advantage of air cooling is its ease of use and ease of use, but the thermophysical properties of air make these systems less attractive. For high-performance electrical engineering, liquid cooling is generally much more efficient than air cooling. This is due to better thermo-physical properties and also to provide a higher heat transfer coefficient than for gases. However, liquid cooling brings risks and potential problems such as leakage, corrosion, increased weight and condensation. Water is most often used for indirect cooling, but direct cooling must use a dielectric liquid due to the requirement for electrical insulation [5].

The cooling system based on the phase change of the working medium is one of the less used cooling technologies. Thermal energy is absorbed or released as the working medium changes its phase. The phase change is usually between gaseous and liquid states. Devices that work on this principle are called heat

tubes. The main disadvantage of this technology is the limited thermal capacity of the liquid phase [5].

### 3 Principle of heat pipe

The heat pipe is a closed two-phase system in which the heat transfer is mediated by circulating the vapor and liquid phases of the working medium between the heated and cooled areas. A schematic representation of the heat pipe is shown in Figure 1. By supplying the heat flux to the evaporating part of the system, the liquid on the inner wall begins to evaporate, then the steam continues to the condensation part, where it starts to condense upon contact with the colder internal environment. The intensity of the heat transfer between the condensation and evaporation part is due to the high value of the heat transfer coefficient in the inner space of the tube during the phase transformations of the working substance. As a rule, the heat pipe comprises a certain inactive adiabatic portion located between the condensation and evaporation portions. The heat pipes can be divided into gravitation, rotary and capillary tubes [6] [7].

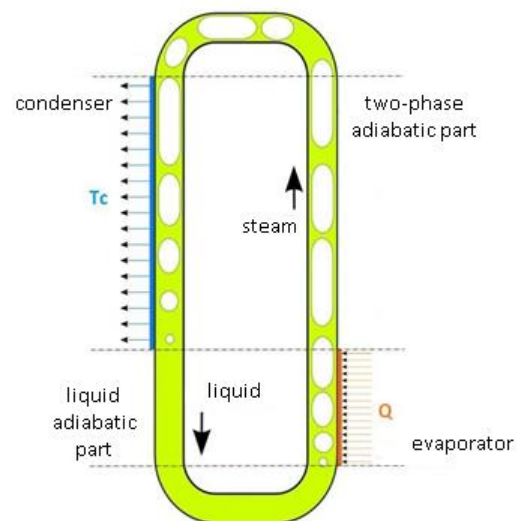


Figure 1 Schematic diagram of a two-phase heat pipe [5]

#### 3.1 Mathematical model

The whole mathematical model is designed to remove heat from the electrical enclosure. Based on the simple measurements performed on the model of the heat pipe, temperatures and pressure were recorded at events that took place in the heat pipe. From these input data, the potential performance of the heat pipe was calculated, which is able to take of the interior cabinet and transfer it to the outside. This calculation of the mathematical model of the heat pipe was performed on the basis of the theoretical relationships

determined for this issue under ideal conditions. The values of physical quantities were determined from the tables based on the measured values of outside temperature and pressure inside the tube. The thermal equilibrium theory between the evaporator and condensation part of the heat pipe was used in the power calculation.

$$\dot{Q}_k = \dot{Q}_v \quad (1)$$

This equilibrium implies that the power drawn at one end of the heat pipe must be equal to the power drawn at the other end. Therefore, the power calculation was chosen for only one part of the heat pipe.

### 3.1.1 Calculation of power on condenser and evaporator

The basic dimensions of the condenser and evaporator of the heat pipe are given in Table 2 and in Table 3.

Table 2 Capacitor dimensions

Name	Symbol	Unit	Value
capacitor length	$l_k$	(m)	0,78
capacitor width	$\check{s}_k$	(m)	0,3
condenser height	$h_k$	(m)	0,3
pipe length	$l_f$	(m)	0,3
number of pipes vertically	$n_\varepsilon$	(-)	10
number of tubes in the whole capacitor	$n_c$	(-)	260
inner pipe diameter	$d_1$	(m)	0,013
pipe external diameter	$d_2$	(m)	0,015
slat spacing	$s_l$	(m)	$250 \cdot 10^{-5}$
lamella height	$h_l$	(m)	0,3
lamella thickness	$\delta_l$	(m)	$25 \cdot 10^{-5}$

Table 3 Evaporator dimensions

Name	Symbol	Unit	Value
outside diameter of pipe	$d_o$	(m)	0,015
inner pipe diameter	$d_i$		0,013
length of the computational element of the lamella	$h_f$		0,050
height of the computational element of the lamella	$b_f$		0,050
lamella thickness	$\delta$		$25 \cdot 10^{-5}$
clearance between the lamellas	$a$		$235 \cdot 10^{-5}$

Table 3 Evaporator dimensions(continue)

Name	Symbol	Unit	Value
entry area of the cross section	$A_o$	(m <sup>2</sup> )	$11,75 \cdot 10^{-5}$
smallest cross area	$A_s$		$8,23 \cdot 10^{-5}$
inner surface of the pipe	$A_i$		1,078
total evaporator surface	$A_c$		39,248
bare tube surface without lamellas	$A_{to}$		1,2438
lamella surface	$A_f$		38,334

The properties of the working medium that need to be changed when changing the heat load or evaporator volume are listed in Table 4 at 25 ° C.

Table 4 Working medium parameters at 25 °C

Name	Symbol	Unit	Value
supply air temperature	t1	(°C)	21
exhaust air temperature	t2	(°C)	29
mean temperature	t	(K)	298,15
kinematic viscosity	$\nu_v$	(m <sup>2</sup> .s <sup>-1</sup> )	1,57.10 <sup>-5</sup>
dynamic viscosity	$\mu$	(Pa.s)	1,87.10 <sup>-5</sup>
thermal conductivity	$\lambda_v$	(W.m <sup>-1</sup> .K <sup>-1</sup> )	0,026
density	$\rho_v$	(kg.m <sup>-3</sup> )	997
the latent heat of evaporation	l <sub>2,3</sub>	(kJ.kg <sup>-1</sup> )	2 441,66

Various heat transfer coefficients on the inside and outside of the condenser tubes were considered in the calculation. Both coefficients had to be recalculated through the relationships in the given case with different filling of the evaporator volume.

In the inner space of the horizontal tubes of condenser, condensation of saturated water vapor took place into liquid. The heat transfer coefficient in this space was calculated from the relation [7]:

$$\alpha_{ki} = 0,56^4 \sqrt{(gl_{3,2} \rho^2 \lambda^3) / (\nu \vartheta d_i)} \quad (2)$$

The outside side of the tube was cooled by forced convection of air from an external fan. The heat transfer coefficient on the outside of the pipe was expressed from a number of interrelated relationships. First, the areas of the slats and tubes. [8]

Minimum external flow cross-section:

$$S_0 = h_k \xi_k - n_c d_2 l_r - \frac{l_r}{s_l} h_l \delta_l \quad (3)$$

Slat area without tubes:

$$S_r = 2l_k h_k - \frac{2n_c \pi d^2}{4} + 2\delta_l h_k + 2l_k \delta_l \quad (4)$$

Surface of the lamella and the free pipe section:

$$S_2 = S_r + \pi d_2 (s_l - \delta_l) \frac{l_r}{s_l} \quad (5)$$

Inner surface of the pipe at the span of the lamella:

$$S'_1 = \pi d_1 s_l \quad (6)$$

Inner surface of the whole pipe:

$$S_1 = \frac{l_r}{s_l} S'_1 \quad (7)$$

Heat transfer coefficient to rib:

$$\alpha_v = 0,223 \frac{\lambda_r}{d_2} \left( \frac{d_2 m_v}{S_0 \mu_v} \right)^{0,65} \left( \frac{s_l}{d_2} \right)^{0,19} \left( \frac{s_l}{h_l} \right)^{0,14} \quad (8)$$

Rib efficiency:

$$\eta_r = \frac{\tanh(m h_l)}{m h_l} \quad (9)$$

$$m = \sqrt{\frac{2\alpha_r}{\lambda_l \delta_l}} \quad (10)$$

Heat transfer coefficient on the outside of the pipe:

$$\alpha_2 = \alpha_r \psi \left( 1 + \left( \eta_r - 1 \right) \frac{S_r}{S_2} \right) \quad (11)$$

To calculate the heat pipe power, the mean logarithmic temperature and the heat transfer coefficient must be calculated.

Mean logarithmic temperature difference:

$$\Delta t_{str} = \frac{\Delta t_1 - \Delta t_2}{\ln \frac{\Delta t_1}{\Delta t_2}} \quad (12)$$

Heat transfer coefficient:

$$k = \frac{1}{\frac{1}{\alpha_1} + \frac{s_l}{S_1} \frac{1}{\alpha_2}} \quad (13)$$

Total heat output dissipated by heat pipe:

$$\dot{Q} = k \Delta t_{str} S_1 \quad (14)$$

The resulting values of the heat pipe performance, which were calculated on the basis of mathematical relations, are listed in Table 5. Calculation was performed at different heat loads and evaporator volume fillings with water.

Table 5 Theoretically calculated heat pipe power

Simulated power [W]	Calculated potential performance				
	20 %	40 %	60 %	80 %	100 %
500	638	640	643	644	648
750	891	895	897	911	913
1,000	1,123	1,134	1,149	1,152	1,154
1,500	1,235	1,237	1,240	1,242	1,246
2,000	1,407	1,416	1,422	1,425	1,441

#### 4 Conclusions

The study points to the theoretical results of cooling efficiency using a heat pipe at various thermal loads and system fill volumes. The results were obtained on the basis of a mathematical model with initial measured parameters.

The results show that theoretically calculated values of heat output have approximately the same values with the amount of simulated heat supplied. At lower thermal loads of 500 W, 750 W and 1,000 W, higher heat dissipation values were calculated using the model. At 1,500 W and 2,000 W simulated power, the heat transfer power was lower. In the mathematical model, the actual capacitor dimensions were assumed and were fixed. Based on these values, the calculation in which the temperature and the pressure in the heat pipe were variable was also developed. All other physical quantities were derived from the temperature-based tables.

The mathematical model gives only theoretical information, which is based on the table values for given temperatures. The results from this model can be compared with the actual amount of heat dissipated from the heat pipe.

#### The reference list

- [1] *The Joule Heating Effect*, 2014-10-31, 2017-02-21, [cit.2019-2-18], [online] <<https://www.comsol.com/multiphysics/the-joule-heating-effect>>.
- [2] *Rittal - tipy na chlazení*, 2017, [cit. 2019-01-25], [online] <[https://www.rittal.com/cz/cs/content/cs/unternehmen/presse/pressemeldungen/pressemeldung\\_detail\\_33920.jsp](https://www.rittal.com/cz/cs/content/cs/unternehmen/presse/pressemeldungen/pressemeldung_detail_33920.jsp)>.
- [3] SLOTNICK, B.: *How to Calculate Heat Dissipation for VFDs*, 2015-08-05, [cit. 2019-01-08], [online] <<https://thermal-edge.com/how-to-calculate-heat-dissipation-for-vfds>>.
- [4] SLOTNICK, B. *How Temperature Control in Electrical Enclosures Affects Component Life* 2017,

[cit. 2019-04-30], [online] <<https://thermal-edge.com/how-temperature-control-in-electrical-enclosures-affects-component-life/>>.

- [5] ANDRJESDÓTTIR, Ó.: *Experimental characterization and optimization of a compact thermosyphon with enhanced boiling surface for power electronics cooling*. Switzerland, Institute of Energy Technology, 2012
- [6] HLAVAČKA, V., POLÁŠEK F.: *Tepelné trubice v elektro-technice*, Praha, Nakladatelství technické literatury, 1990
- [7] SAZIMA, M.: *Sdílení tepla*, Praha, Nakladatelství technické literatury, 1993
- [8] PILAŘ, A., NÝVLT, J.: *Chemické inženýrství III. Difúzní operace*, Praha, Nakladatelství technické literatury, 1972

#### Acknowledgement

This work has been supported by the projects APVV-17-0311 “Research and development of zero waste technology for the decomposition and selection of undesirable components from process gas generated by the gasifier” and KEGA 033ŽU-4/2018 “Heat sources and pollution of the environment”.